Electric Field Poling Effects on the Molecular Reorientational Dynamics of Side-Chain Nonlinear Optical Polymers

Hanlin Wang, Richard C. Jarnagin,* and Edward T. Samulski*

Department of Chemistry, The University of North Carolina at Chapel Hill, Chapel Hill, North Carolina 27599-3290

Received December 7, 1993; Revised Manuscript Received March 17, 1994®

ABSTRACT: The molecular reorientational dynamics of the side-chain nonlinear optical (NLO) polymer [poly(methyl methacrylate-*co*-*p*-nitrophenylprolinol)] were investigated. A nonlinear optical response, second-harmonic generation (SHG), was used to probe the induction and decay of molecular orientational order. A two-mode growth of the SHG signal induced by the poling field at temperatures above T_g and a subsequent two-mode SHG relaxation in the absence of the poling field at temperatures below T_g were observed. A qualitative interpretation that distinguishes between the motion of the side-chain NLO chromophores decoupled from polymer segmental movement and the motion of the chromophores coupled to the polymer segmental movement was proposed to explain the observed two-mode poling and relaxation phenomena. Under the influence of an electric poling field, after a rapid response of the side-chain chromophore, the polymer chain contour rearranges itself and creates an anisotropic local environment. This field-induced anisotropic local environment in turn enhances the orientational ordering of the NLO chromophores and also significantly influences the relaxation behavior after the poling field is removed. A poling field-jump experiment gave direct evidence that the polymer backbone undergoes anisotropic rearrangement during the poling process. The significant influence of the field-induced polymer backbone rearrangement on the SHG relaxation behavior was manifested in a correlation experiment contrasting the poling process and the SHG relaxation behavior.

1. Introduction

The structural and dynamic complexity of condensed phases of polymers continues to challenge polymer scientists. One aspect of this challenge is understanding molecular motions in the polymer solid state because those motions dictate the relaxation of most macroscale physical properties of polymeric materials.[1,2] A related aspect of this challenge is the recent search for useful second-order nonlinear optical (NLO) polymeric materials. Both doping a polymer matrix with hyperpolarizable molecular chromophores and covalently attaching such chromophores to polymer chains have been explored in the context of the NLO phenomenon, such as second-harmonic generation (SHG).[3,4] Chromophores possessing large hyperpolarizabilities can impart significant NLO properties to an inert polymeric material provided that (1) the isotropic symmetry of chromophore orientational distribution can be broken and (2) the resulting asymmetry once established can be maintained. The establishment of an asymmetric environment is a rigorous requirement because of the third-order tensorial property of the second-order response.[4] This asymmetry is commonly achieved by the process of electrical field poling, a technique that has been described in much detail elsewhere.[4,5]

The asymmetric orientational distribution of NLO chromophores created in the presence of a poling field tends to relax toward the isotropic state in the absence of the poling field. Poled polymer films can have significant rates of relaxation even at temperatures well below the glass transition temperature (T_g).[6-11] Long-term stability of the asymmetric order is essential for applying these materials in real NLO devices.[4] Understanding the chromophore relaxation mechanism can help realize the goal of long-term NLO stability, and, moreover, the methodology used to monitor relaxation can also be of general utility in understanding the nature of dynamics in the polymer solid state. Specifically, the sensitivity of NLO responses such as SHG is ideally suited for observing the motional dynamics associated with the relaxation of anisotropic order independent of intended applications. When a certain type of NLO chromophore that serves as a probe of this anisotropy is incorporated into the polymer matrix by either doping or covalently attaching to the polymer backbone, detailed information about the polymer conformation and mobility can be determined. The local polymer conformation and mobility govern the chromophore's local environment and therefore influence its relaxation behavior. By monitoring the SHG signal versus time, new insight into the motional dynamics of the chain and chromophore may result.

There is a growing body of research that reports and analyzes the decay of the SHG signal for both doped guest–host systems and covalent side-chain systems.[6-11] Two functions are often used for fitting SHG decay data after removal of the poling field: the Kohlrausch–Williams–Watts (KWW)[12] stretched exponential

$$f(t) = Ae^{-(t/\tau)^{\beta}} \tag{1}$$

or a biexponential function

$$f(t) = Ae^{-(t/\tau_A)} + Be^{-(t/\tau_B)} \tag{2}$$

A quantitative fit of SHG relaxation data to the stretched exponential (eq 1) implies a single relaxation mode with a distribution of relaxation times. In contrast, a fit to the biexponential (eq 2) implies that two distinct modes of motion are operative. Both fitting functions have been employed in the literature.[6-8,10] A number of interpretative viewpoints based on free volume and free-volume distribution,[6] on hetereophase and interfacial diffusion of defects,[8] etc., have also been presented. Several additional effects on relaxation behavior, such as thermal history of the sample and physical aging, have also been reported.[6,8,11] Surprisingly, less attention has been paid to the electric field poling history of the sample and the possible correlation between the behavior of the growth of the SHG

* To whom correspondence should be addressed.

® Abstract published in *Advance ACS Abstracts*, July 15, 1994.

0024-9297/94/2227-4705$04.50/0

signal in the poling field and the behavior of subsequent relaxation after removal of the field.

The present paper deals with the orientational dynamics of copolymers bearing NLO active pendant side-chain chromophores: poly(methyl methacrylate-*co*-*p*-nitrophenylprolinol) (PMMA–NPP).

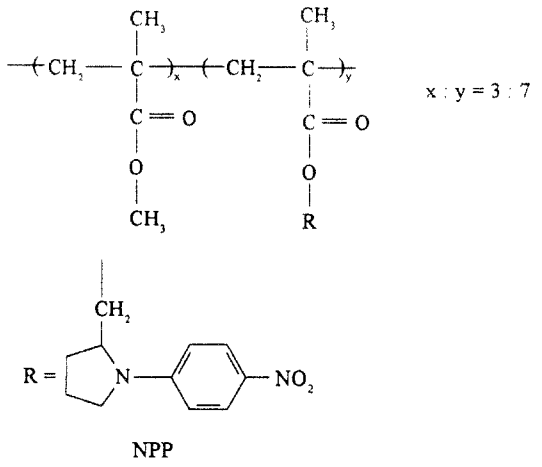

NPP

The anisotropic orientation of the side-chain NPP chromophores and the relaxation of that anisotropy was probed by SHG measurement. Corona poling was used to establish the initial asymmetric orientation distribution of chromophores. Molecular orientational dynamics manifested in the growth of the SHG signal induced by the poling field at elevated temperatures, and the subsequent SHG relaxation in the absence of the poling field at lower temperatures, was investigated. A qualitative mechanism based on the observation of the direct correlation between the initial growth of the SHG signal and the subsequent relaxation behavior is proposed. A field-jump experiment for testing the mechanism was designed, and the results were fully consistent with the proposed mechanism.

2. Experimental Section

Several poly(methyl methacrylate-*co*-*p*-nitrophenylprolinol) polymers were synthesized with different NPP substitutional levels. The synthetic strategy was formation of copolymers between methyl methacrylate (MMA) and methacryloyl chloride at different monomer ratios and their subsequent conversion to the ester with *p*-nitrophenylprolinol (NPP). The detailed synthetic procedure is given elsewhere.[13] The data in this paper were obtained with the polymer containing a 7:3 ratio of NPP–methacrylate to MMA. The T_g of the polymer is 167 °C as determined by differential scanning calorimetry (DSC). Appropriate amounts of the polymer were dissolved in *N*-methylpyrrolidone (NMP) to form a solution of about 2 wt % concentration. Undissolved particles were removed by centrifugation. Films of good optical clarity were not obtained by the spin-coating method. However, optically clear films were prepared by casting the solution on ITO glass microscope slides and slowly evaporating the solvent in a restricted atmosphere at 50 °C for 5 days. The films were then annealed in a vacuum oven at 167 °C for 24 h. The films prepared by this solution-casting method are visually clear, and the thickness ranges from 3 to 4 μm as determined by an M-line waveguide technique (Metricon Model 2010 prism coupler). A polymer film with about 5 wt % NPP doped in the PMMA matrix was also prepared by the same method. The T_g of the doped films is about 90 °C as determined by DSC. The absorption spectra of these films were measured on a UV/vis spectrophotometer (Perkin-Elmer Lambda 6). The maximum absorption occurs at 390 nm, and the absorption edge is about 480 nm. There was insignificant optical absorption at either 1064 or 532 nm.

The annealed film was mounted on a rotatable heating stage for control of the incidence angle of the laser beam. The geometric arrangement of the sample holder, the corona poling tip, and the laser beam in the incident plane cross section is shown in Figure 1A. The film was heated by a built-in foil heater with an open hole at the center (about 1 cm in diameter), and its temperature was controlled by a RTD type temperature controller with ±0.5 °C accuracy. The corona discharge was generated by a sharp tungsten needle held normal to the polymer film and biased with a high negative static potential across a 2.0-cm air gap. Unless specified, the discharge voltage used in this work was 10 kV (the Townsend discharge threshold was about 2.5 kV).

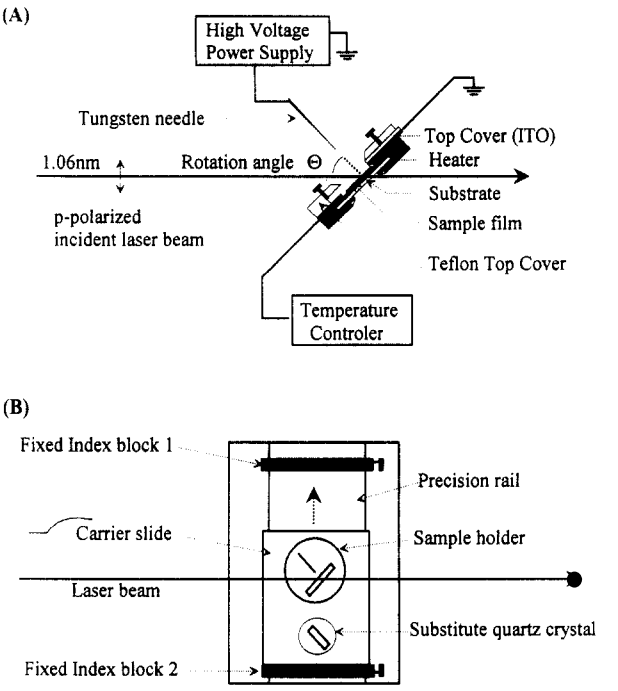

Figure 1. (A) Geometric arrangement of the sample holder, the corona poling setup, and the laser beam. (B) Top view of the sample channel. The sample and the substituted quartz crystal can be switched with each other into the measurement track by moving the carrier slide along the precision rail. The relative positions of the sample and the quartz crystal to the laser beam can be controlled by adjusting the positions of the two index blocks on both sides of the rail.

A p-polarized collimated beam of about 1-mm diameter from a Nd:YAG laser (1064-nm wavelength, 10-ns pulse duration, and 0.4 mJ/pulse; Q-switched at 10 Hz) was divided into two channels. One channel contained a quartz crystal (110) (d_{11} = 0.45 pm/V)[14] to provide a second-order signal for pulse-to-pulse normalization of laser flash intensity fluctuations. The second channel contained the sample on the heating/poling stage and could be substituted by a second quartz crystal through an accurate transverse slide rail (Figure 1B). The angle of the quartz crystal in the sample channel relative to the laser beam was fixed. The sliding substitution of the quartz crystal for the sample provides a calibration for the measurement of the SHG intensities from different samples at different times. The angle between the laser beam and the polymer sample surface was fixed at 52°. The SHG signals from both the reference channel and the sample or standard channel were observed simultaneously by two monochromators and monitored by photomultipliers and boxcar averagers in real time. The boxcar output was stored in a PC through a GPIB (Metra Byte) and SR245 (Stanford Research) interface. Signal processing and curve fitting were executed separately. The integration gate window for each laser pulse was triggered by a photodiode sampling a small fraction of the laser pulse. The data acquisition, analysis, and experiment control were provided through programs written in ASYST (Macmillan Software). Each data point represents the average of three pulses of the SHG signal at 532 nm.

Measurement of the growth of the SHG signal during corona poling was done at a series of sample temperatures according to the following sequence. First the sample was heated 5–10 °C above T_g for several minutes until all the residual SHG disappeared. Then the temperature was set to the desired value, and

the sample was allowed to thermally stabilize (~10 min was required). The fundamental incident light at 1064 nm was turned on and a base line established. The poling field was then applied, and the growth of the SHG signal was monitored in real time. At the end of each measurement, the poling field was turned off and the residual SHG signal was removed by resetting the sample temperature above T_g for a few minutes. After the SHG signal decayed to the base-line value, the sample was cooled to a new temperature and the measurement cycle was repeated.

Each measurement of SHG relaxation was carried out in the following way: The poling field was turned on with the sample held at a desired temperature. After the SHG intensity reached a constant value for these conditions, the sample was cooled at about 4 °C/min to a lower temperature (at which the relaxation measurement was to be carried out) and maintained at that temperature for about 10 min. The corona voltage was then turned off, and the surface charge that builds up on the sample during corona poling was manually discharged by placing a grounded ITO slide above the polymer surface and pressing to make firm contact with the sample. This sliding ITO glass discharge plate was mounted inside the sample holder and thus is at the same temperature as the sample. This process only takes several seconds and is effective in removing the corona-produced surface charge density that establishes the poling field. This discharge procedure precludes the measurement of the SHG relaxation within the initial 5–10 s. The decay of the SHG intensity was then continuously monitored on a minutes to hours time scale.

3. Results

An isotropic film subject to an electric poling field in the direction perpendicular to the film surface converts energy into transmitted second-harmonic power density $I^{2\omega}$. When the fundamental beam is p-polarized and incident on the film with a nonlinear optical coefficient $d = (1/2)\chi^{(2)}(-2\omega;\omega,\omega)$, the converted second-harmonic intensity is given by:[15]

$$I^{2\omega} = \frac{(8\pi)^3}{c}(I^{\omega})^2\left[\frac{T_{2\omega}(\theta)}{(n_{\omega}^2 - n_{2\omega}^2)}\right](d_{31}\cos^2\theta'_{\omega}\sin\theta'_{\omega} - d_{33}\sin^3\theta'_{\omega})^2\sin^2\left(\frac{\pi l}{2l_c}\right) \quad (3)$$

Here c is the velocity of light in vacuum and l is the sample thickness; I^{ω} is the power density of the fundamental beam inside the medium. $T_{2\omega}$ is the transmission factor which depends on the incident angle and the refractive indices of the material at fundamental (n_{ω}) and at second-harmonic ($n_{2\omega}$) frequencies. The quantity l_c is the correlation length which is given by $l_c = \lambda/4(n_{\omega}\cos\theta'_{\omega} - n_{2\omega}\cos\theta'_{2\omega})$, where θ'_{ω} and $\theta'_{2\omega}$ are the angles of refraction of the fundamental and the second-harmonic beams, respectively. They are related to the incident angle θ by Snell's law. The d_{31} and d_{33} are determined by:[4a,c]

$$d_{31} = B(\langle\cos\phi\rangle - \langle\cos^3\phi\rangle) \quad (4)$$

and

$$d_{33} = D\langle\cos^3\phi\rangle \quad (5)$$

Here B and D are quantities proportional to local field factors, molecular hyperpolarizability, and the number density of the chromophores. ϕ is the orientational angle between the chromophore and the poling field.

For quantitative data analysis, one might need to consider the poling field induced birefringence (Kerr effect[16]) which depends on the chromophore's orientational order parameter. This complicates the quantitative data analysis of SHG induction and decay. But in many cases,

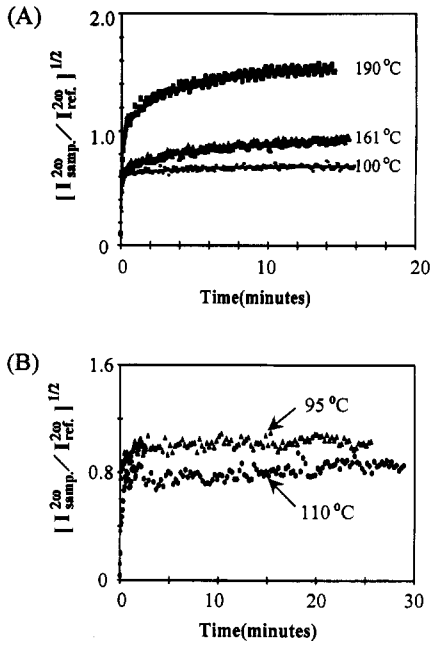

Figure 2. Corona poling field-induced growth of the SHG signal from two different samples. (A) The SHG response of the sample (T_g = 167 °C) with the NPP chromophores (70 mol %) covalently attached to the PMMA backbone as side chains. (B) The SHG response of the sample (T_g = 90 °C) with the NPP chromophores doped (5 wt %) into the PMMA matrix; the poling temperatures are indicated.

electric-field-induced birefringence Δn_{ind} in amorphous polymer systems is on the order of 10^{-2}–10^{-3} and for qualitative analysis, it can be neglected.[17-19] Then the refractive indices in the expressions for the coherence length l_c and transmission factor $T_{2\omega}$ can be treated as constants. In the weak poling field condition, as applied to the present case, one has $d_{31} \cong (1/3)d_{33} = (1/3)D\langle\cos^3\phi\rangle$. Therefore, for a sample subject to a fundamental beam with constant intensity at fixed incident angle, the transmitted SHG intensity can be expressed as:

$$I^{2\omega} \propto \langle\cos^3\phi\rangle^2 \quad (6)$$

Thus, the SHG induction and decay curves reflect the chromophore's polar orientational induction and decay due to molecular reorientation.

3.1. Growth of Orientational Polarization under the Poling Field. The external electric-field-induced growth of the SHG signal from the sample with the NPP chromophores (70 mol %) covalently attached to the PMMA backbone and subjected to a constant corona discharge is shown in Figure 2A for three different temperatures: 190, 161, and 100 °C. In each case the vertical axis is the square root of the SHG intensity of the sample normalized to a substituted quartz reference in the same channel (see Figure 1B) and is thus proportional to the nonlinear optical polarization of the sample. Qualitative examination of Figure 2A shows that the growth of the polarization follows a two-component process at temperatures above or close to the sample T_g of 167 °C: an initial fast response to the poling field followed by a much slower response. The growth of the polarization was fitted to a biexponential:

$$\left(\frac{I_{sample}(2\omega)}{I_{reference}(2\omega)}\right)^{1/2} = A(1 - e^{-t/\tau_A}) + B(1 - e^{-t/\tau_B}) \quad (7)$$

In Table 1 are listed the optimized values of the fitted parameters at various temperatures over the range from

Table 1. Parameters Obtained by Fitting the Square Root of the Growth Intensities of the SHG Signal in Figure 2A to eq 7

T (°C)	τ_A (min)	A	τ_B (min)	B	σ
55	0.028	0.55	1.91	0.056	0.017
100	0.024	0.62	4.22	0.081	0.018
136	0.039	0.61	5.05	0.17	0.021
151	0.049	0.67	6.53	0.22	0.022
161	0.057	0.66	5.46	0.28	0.022
167	0.074	0.61	4.43	0.36	0.022
174	0.036	0.81	3.42	0.48	0.030
190	0.052	1.01	3.23	0.52	0.035

55 to 190 °C. The comparison of the observed data with the curves (solid lines) calculated by eq 7 using the parameters given in Table 1 is also shown in Figure 2A. The physical significance of the fitting parameters will be discussed later in this paper.

The electric-field-induced growth of the SHG signal from the NPP-doped (5 wt %) PMMA sample is shown in Figure 2B. The sample was poled at two different poling temperatures, 95 and 110 °C (5 and 20 °C, respectively, above the sample T_g of 90 °C), using the same corona voltage as was applied in case A. In contrast to the case of side-chain NPP (case A), the SHG signal from the sample doped with solute NPP (case B) rose rapidly and reached stable limiting values in a very short period of time at both temperatures. It was also found that the magnitude of the SHG signal from the sample poled at 110 °C is slightly lower than that poled at 95 °C.

3.2. Relaxation of Orientational Polarization. To distinguish effects of orientational relaxation after the corona poling source is turned off from effects associated with slow leakage of surface charge density accumulated during corona poling, one must have a way to rapidly discharge the surface. Several methods have been used. They include washing the film with selected solvent after the corona source is turned off,[20] aging the film at room temperature for various periods of time before doing relaxation measurements,[8] and using a surface voltage detector to monitor the decay of the surface potential for inclusion of its effect in the subsequent data analysis.[10] All of these methods have a time delay between removal of the corona source and onset of the observable relaxation. Contact poling is a proven method for discharge of surfaces although it often initiates dielectric breakdown and limits the magnitude of the poling field which can be applied.[4]

In this research a simple technique was used to remove the sample internal electric field created by corona discharge. After the SHG signal reached its steady state under the poling field, an ITO glass plate (held at the sample temperature) was quickly slid between the corona discharge and sample polymer film and tightly pressed into contact with the top of the film, with its conducting surface facing the charged sample surface. When the conducting surface of the top ITO glass was properly grounded, the charge deposited on the top of the sample surface was neutralized immediately. The internal field created by the trapped charge beneath the sample surface will also be canceled by the corresponding image charge inside the ITO conducting layer. The field created by the small amount of bulk charge will also be reduced by the image charge inside the ITO layer. Figure 3 shows the effectiveness of this method. In both cases A and B of Figure 3, the film was poled at 190 °C. The relaxation was also monitored at 190 °C because the rapid decay of the SHG signal above T_g on the removal of the poling field provides an effective way to monitor the decrease of the internal electric field. For case A the SHG relaxation was continuously monitored after the second ITO plate was slid on top of the film and contacted with the sample, leaving the corona voltage on. In case B the SHG relaxation was continuously recorded after the corona voltage was turned off without sliding the ITO discharge plate into place. It is clear that in case A the SHG signal relaxed to zero much faster than in case B. This observation shows that most of the surface charge density (and the resulting poling field) can be effectively removed in a short period of time (without significant disturbance to the system) by properly grounding the conducting surface of the top ITO plate.

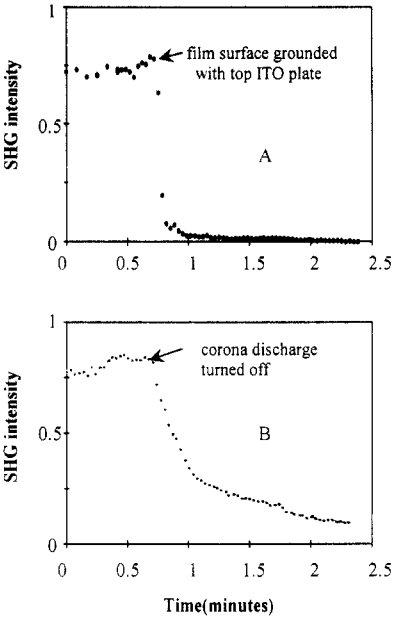

Figure 3. Removal of the film's surface charge built up during the corona poling process. In case A the film's internal electric field was quenched by grounding the sample surface via the top cover ITO plate—sliding it on top of the sample—without turning off the corona discharge. In case B the film's internal electric field was allowed to dissipate of its own accord following removal of the corona discharge. The poling temperature was 190 °C in both cases.

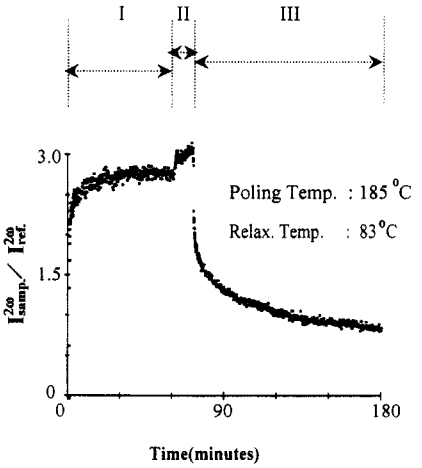

Figure 4. Real-time *in situ* electric field poling and the subsequent relaxation processes. The sample was poled at 185 °C in period I and then gradually cooled to 83 °C in the presence of the poling field in period II. At the end of period II the poling field was removed and the decay of the SHG signal was continuously monitored at 83 °C in period III.

Figure 4 illustrates the real-time *in situ* poling and relaxation process employing the methods described. The sample was poled at 185 °C during period I and cooled down to 83 °C during period II while maintaining the corona discharge, and then at the end of period II, the

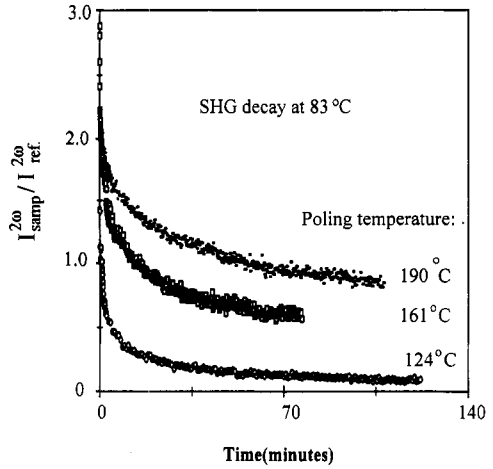

Figure 5. Decay of the SHG signal from the same sample of the NPP side-chain polymer at the same temperature (83 °C). The different decay curves correspond to poling the sample at different temperatures.

poling field was turned off by the surface discharge method and the decay of the SHG signal was continuously monitored during period III. The SHG signal increased significantly when the sample was cooled from 185 °C to the temperature just below T_g while maintaining the corona discharge (at the beginning of period II). The increase was attributed to a decrease in the sample conductivity and the resulting increase in the sample internal field. The SHG signal increased even more when the sample was further cooled to 83 °C, but this poling behavior is still not well understood and a detailed study is in progress. The initial immediate drop of the SHG signal after the removal of poling field contains a contribution from the loss of the fundamental intensity via reflection and absorption of the top ITO discharge plate. A part of the fast decay component may also be contributed from the loss of the electronic part of the electric-field-induced SHG (EFISH) signal which is a third-order NLO phenomenon and has little relation to the molecular reorientational motion. The subsequent slow decay of the SHG signal (Figure 4) during period III resulted from the relaxation of the field-induced NLO chromophore's polar order.

In Figure 5 are shown three relaxation curves obtained from the same sample at the same temperature (83 °C): each curve shows the intensity of the SHG signal relative to the substituted quartz reference in the same channel. The initial SHG intensities of the three curves were induced by the same corona poling voltage for the same period of time (20 min). The major distinction among the three relaxation curves is that three different poling temperatures were used: The upper curve corresponds to poling the sample at 190 °C (above T_g), the middle curve results from poling at 161 °C (just below T_g), and the lower curve corresponds to poling at 124 °C (well below T_g). The significant result from this series of relaxation curves is the magnitude of the residual SHG intensity at long times: The long-time residual orientational order was clearly larger when the sample was poled at higher temperatures.

The data illustrated in Figure 6, panels A–D, show orientational relaxation of the same film at four different temperatures, 81, 102, 124, and 137 °C. In each case the poling temperature was 167 °C (equal to T_g) and the poling time was 40 min. Note that the vertical axis represents the square root of the relative SHG intensity which is proportional to the NLO polarization. The solid lines are the result of fitting the data to a stretched exponential

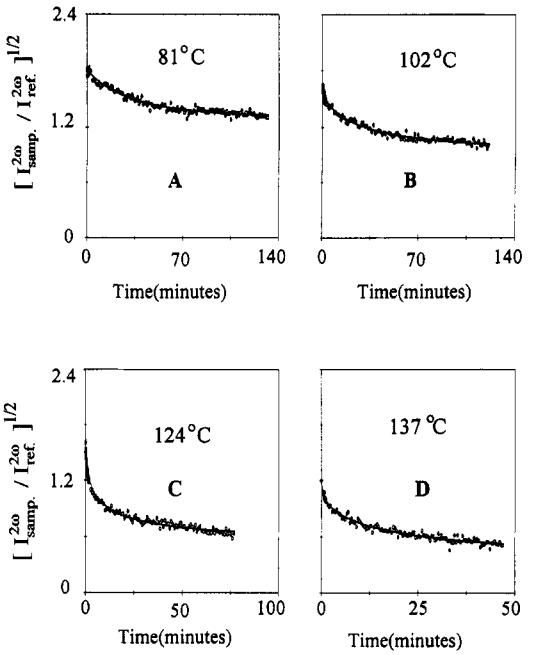

Figure 6. Relaxation data from the NPP side-chain sample obtained at 81, 102, 124, and 137 °C, respectively. The solid lines represent the fitted results using eq 8 and the fitting parameters are given in Table 2.

Table 2. Parameters Obtained by Fitting the Square Root of the SHG Decay Curves in Figure 6 at Various Temperatures to eq 8

T (°C)	τ (min)	B	C	β	σ
81	37.5	0.50	1.29	0.85	0.025
102	27.1	0.73	0.95	0.55	0.027
124	14.9	0.91	0.53	0.45	0.024
137	19.7	0.88	0.32	0.44	0.027

plus a constant:

$$\left(\frac{I_{\text{sample}}(2\omega)}{I_{\text{reference}}(2\omega)}\right)^{1/2} = A\exp[-(t/\tau)^{\beta}] + C \qquad (8)$$

The fitting parameters A, τ, β, and C are listed in Table 2. Clearly a significant residual orientation persists in each sample with its magnitude, as well as its rate of relaxation, dependent on the temperature. Relaxation continues at a very slow rate over many days. These very slow relaxation modes are lumped into an effective constant C for fitting the SHG relaxation on the observation time scales reported here. Thus the data show at least two modes for relaxation of chromophore orientation, a fast mode and a very slow mode.

4. Mechanism of Electric Field Poling and Relaxation Dynamics

Four theoretical models have been used to calculate the degree of orientation of the NLO dipole chromophores in the polymer matrix under a poling field: (1) the isotropic model,[4a,5] (2) the Ising model,[3,4a] (3) the Singer–Kuzyk–Sohn (SKS) model,[21,22] and (4) the extended Maier–Saupe mean-field model.[23,24] The isotropic model simply treats the media as an isotropic medium, and the potential energy of the system is equal to the interaction energy of the NLO dipoles with the applied electric field (including the local field correction). This interaction energy is only dependent on the orientation of the dipoles relative to the applied field. The other three models deal with anisotropic media (liquid crystal phases), so that the potential is dependent on the orientation of the NLO dipoles relative

to both the local axial direction in the medium and the applied field direction. Since all these models only deal with thermodynamic equilibrium states, they are not suitable for describing the electric field poling dynamics. However, one useful conclusion can be drawn from the above models: field-induced polar ordering of NLO dipoles can be enhanced by intrinsic axial ordering in liquid crystalline phases.[4d,24]

We begin our analysis by considerating the differences observed in the poling field-induced growth of the SHG signal at different temperatures. As is demonstrated in Figure 2A the growth of NLO polarization in the side-chain sample under a poling field exhibits two modes at temperatures above or close to T_g, a fast growth mode and a slow growth mode. In order to interpret the observed poling behavior, the surface charge effects have to be distinguished; they can be divided into two categories: first, a surface charge accumulation process as the corona discharge was initially applied; second, when the sample was poled more than once, the residual charge trapped inside the sample will influence the subsequent poling.

Moreno and Gross[25] indicated that a certain period of time is required to allow the surface charge density to buildup in a corona poling process. In order to distinguish the slow step growth of the SHG signal as shown in Figure 2A from the effect of possible slow accumulation of surface charge density during the corona poling process, the field-induced growth of the SHG signal from a sample with the NPP chromophores present as a solute guest in the PMMA matrix was also measured under the same corona poling conditions (the same poling voltage, the same tip to surface distance, and also, at the same temperatures relative to the T_g of the doped sample). Compared with the NLO side-chain polymer sample, the SHG signal from the NPP-doped sample responds more rapidly to the changes of the internal poling field due to the effective decoupling of the motion of NPP chromophores from polymer segmental motion. Hence, the NPP-doped sample can serve as a probe to detect the changes of the internal field during corona discharge. As shown in Figure 2B, in contrast to the poling behavior shown in Figure 2A, the SHG signals for the NPP-doped sample reached their stable levels soon after an initial rapid growth. This poling behavior indicated that for our corona poling setup, the internal poling field attains its stable saturation level in a short period of time. Thus, the subsequent slow growth of the SHG signals shown in Figure 2A is attributed to slow improved alignment of the chromophores under the quickly established (but constant) internal poling field. Such a two-mode growth of the SHG signal from side-chain NLO polymers under corona poling was also observed by Eich et al.,[17] but they simply related it to surface charge accumulation; no special attention was paid to this unusual poling behavior.

It has been shown that[10,11] some residual charge trapped inside the film will persist in the film for a long period after the corona voltage is turned off. If the same sample is poled more than once, this residual charge may influence the subsequent poling. In order to eliminate the residual charge effect on the poling behavior, each time before the poling field was applied, the sample was thermally annealed above T_g for several minutes to erase the residual SHG induced by the previous poling. When the SHG decayed to zero, the sample was adjusted to a certain temperature and the poling was repeated. Recently, surface voltage decay measurements indicated that the surface voltage decay is slower than the decay of the SHG signal.[10] At temperatures above T_g, the sample may still have residual charge even when no further SHG is observed. However, as we have demonstrated in our corona poling setup, the electric poling field can reach its stable value much faster than the growth of the SHG signal when the corona voltage is applied even though the magnitude of the sample internal field may be slightly different when the sample was poled more than once. So that, the growth of the SHG signal on our observation time scale can be considered to take place under a constant poling field. In fact in our experiments we did not observe any differences in poling behavior between the first poling and the subsequent poling on the same film at the same temperature as long as the residual SHG was erased by annealing the film above T_g.

As shown in Figure 4 the relaxation is also dominated by a two-mode process. The two-mode relaxation of the SHG signal from side-chain NLO polymers has also been observed by other research groups.[6,8] Models describing the pathways for relaxation of chromophore orientational polarization have been proposed.[6,8,10,11] These models were based on the concepts of free volume and free-volume diffusion and were originally used by Curro, Lagasse, and Simha[26] to explain the physical aging phenomenon in glassy polymers. Lindsay[8] proposed that higher density "grains" were formed in the polymer matrix as the sample cooled down from the "melt" to a temperature well below T_g and that the free-volume diffusion in this hetereophase matrix dominates the long-term relaxation behavior. But prior models have paid little attention to the correlation of a multimode poling process with a subsequent multimode relaxation process nor have they differentiated behaviors between doped and covalently-link chromophore systems.

4.1. Proposed Mechanism: Poling Dynamics. The mechanism proposed here derives in part from two extreme instances of polymer chain segmental orientation: deformed elastomer networks and side-chain liquid crystalline polymers (LCPs). In the first instance,[27-29] segmental order is rather low (quadrupolar order parameters $\langle P_2(\cos\theta)\rangle \approx 10^{-3}$–$10^{-4}$). Nevertheless, there is NMR evidence[27,28] for intermolecular segment–segment and segment–solute interactions that enhance the strain-induced segment orientation. The network chain segments experience extra orientational order via local, anisotropic, excluded-volume ("nematic-like") interactions.[27] In the other extreme is the intrinsic order in the mesophase of LCPs. For side-chain LCPs the pendant mesogenic groups are well-aligned ($\langle P_2(\cos\theta)\rangle \sim 0.5$), and this side-chain order in turn influences the local polymer chain contour[30] which is manifested in scattering experiments:[31,32] the radius of gyration tensor is anisotropic, prolate, or oblate, depending on the mesophase type. The primary feature of these two extreme examples of anisotropic polymer segmental orientation—evidence for intermolecular segment–segment, segment–solute, or segment–side-chain orientational correlation—is the starting point for an E-field-induced orientation mechanism in the melt and glassy states of the NLO polymers considered here.

When the poling field is first applied, an initial fast growth of the SHG signal is partly due to the fast reorientational response of the polar side-chain chromophores. Therefore, a nonzero polarization is rapidly created and its magnitude depends on the size of the local free volume around each chromophore, on the degree of the decoupling between the chromophore and the polymer backbone, and on the poling temperature which determines the thermal fluctuation energy. Since the chromophore dipoles tend to orient along the direction of the poling field, those polymer segments coupled to the chromophores

are subjected to local intra- and intermolecular interactions and respond by changing their conformation locally to adapt to the anisotropic orientation distribution of the poled chromophores. The result is the creation of orientationally biased chain contours among the poled chromophores. In turn, this local anisotropy can enhance the polar ordering of the chromophores (and the SHG intensity), a phenomenon consistent with the SKS model and the extended mean-field model. However, this local environmental anisotropy develops slowly because of the high viscosity limiting the polymer chain conformational rearrangements. Therefore, enhanced local orientational order of chromophores resulting from a more compatible, uniaxial disposition of chain contours develops throughout the poling process and finally reaches a new equilibrium state exhibiting a higher SHG signal. Accordingly, the slow growth of the SHG signal in the poling process is associated with the reorientational motion of polymer backbone chain segments.

Based on this mechanism for the poling process, an appropriate fitting function should be consistent with a two-mode process. We found a biexponential function (eq 7) was appropriate to describe the growth of the SHG signal. In such fits the parameter "A" represents the maximum contribution of the fast growth component with time constant τ_A; its magnitude depends on the strength of the poling field and the chromophore's local mobility. The local mobility is controlled by the size of the free volume around each chromophore, the strength of the coupling interaction between the chromophore and the polymer backbone, and the temperature. The parameter "B" represents the maximum contribution of the slow growth component with time constant τ_B; its magnitude depends on the coupling interaction between the chromophore and the polymer segments and the polymer segmental mobility. The time constants τ_A and τ_B are approximately independent of the strength of the poling field and should be intrinsic parameters of the system. The sum of the saturation limits ($A + B$) for each contributing component represents the maximum obtainable SHG signal at the particular temperature and field values and, therefore, represents the overall poling efficiency under these conditions.

One way to support the proposed mechanism is to inspect the poling process at temperatures well below the T_g. Since polymer chains do not undergo significant reorganization in the glassy state, the slow step growth will be eliminated from the SHG signal and it will level off at a value less than the maximum attainable value in a short period of time. The results presented in Figure 2A are consistent with this description. A second way to test this mechansm is to interrupt the poling process. Figure 7 shows the results of a field-jump experiment designed to probe the proposition that the polymer chain contour rearranges to accommodate the oriented chromophore during the poling process. Throughout the measurement, the poling temperature was kept at 190 °C. As in the case shown in Figure 2A the growth of the SHG signal between t_A and t_B to its saturated value ($I \approx 1.3$; Figure 7) occurs on two different time scales (~10 s and ~10 min). At t_B the corona voltage was turned off for an interval of about 5 s; the SHG signal relaxes to a lower value ($I \approx 0.5$) virtually instantly. In so far as the SHG intensity is a measure of the statistical distribution of chromophore orientation, the $I \approx 0.5$ value right after t_A and the $I \approx 0.5$ value directly following t_B correspond to identical states of chromophore orientational distribution. However, it is clear that when the corona voltage was restored at t_C, the saturated SHG

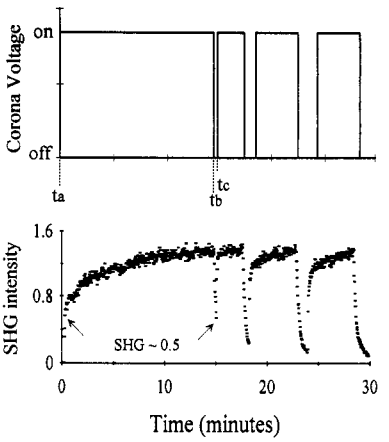

Figure 7. Field-jump experiment for probing the changes of the chromophore local environment during the poling process. The poling temperature was 190 °C.

intensity was recovered almost immediately. This SHG recovery process is very different from the initial SHG growth process after t_A (from $I \approx 0.5$ to the saturated value when the corona voltage was first applied). This difference in the rate of SHG growth was interpreted in terms of very different chromophore local environments (polymer chain conformations). Initially (at $t \approx t_A$) an essentially isotropic, unperturbed environment was present. During the subsequent poling period (t_A to t_B) the local environment shifted to conform to the oriented chromophores. Since the interval between t_B and t_C was too short for a polymer chain contour to undergo significant rearrangement, the growth of SHG following restoration of the poling field at t_C occurs in an environment conducive to a polarized chromophore orientational distribution and, consequently, proceeds much more rapidly than the initial growth in the unperturbed, isotropic environment. Increasing the interval without the corona voltage at this elevated temperature allows the anisotropic polymer chain contours to relax, and there should be a corresponding influence on the subsequent SHG recovery rate when the voltage is reapplied. That expectation was borne out in the observations of Figure 7 taken with longer relaxation intervals.

4.2. Proposed Mechanism: Relaxation Dynamics. The above poling dynamics study indicated that, if the poling temperature is above or close to T_g, not only do the NLO chromophores undergo reorientational motion but the polymer chain contour also rearranges in the poling field. As a result, a local uniaxial environment that facilitates further alignment of the NLO chromophores is created during the poling process. When the polymer is cooled down to a temperature well below T_g, the anisotropic orientational distribution of the chromophores and their anisotropic local environment are both frozen in. The subsequent slow chromophore reorientational relaxation not only is dependent on the size of the free volume in the vicinity of a chromophore and the rate of free-volume diffusion but is also strongly coupled to the relaxation of its local anisotropic environment. This latter process is mainly controlled by cooperative motion of polymer segments.

On the basis of this mechanism, we can give a qualitative description of the SHG relaxation pathway in the glassy state after removal of the poling field. The relaxation of the SHG signal exhibits three different steps after removal of the poling field: (1) an initial fast decay; (2) an intermediate slow decay; (3) a final very slow decay. As demonstrated in Figure 4, similar to the poling process, the initial fast decay of the signal (excluding the immediate drop due to surface discharge and attenuation of the signal

by the discharging ITO plate) is attributed to the existence of some degree of freedom for the chromophores to rotate. This depends on the size of the free volume in the vicinity of each chromophore and also depends on the coupling interaction—through bond and through space—between the chromophores and the polymer backbone. Consistent with the free-volume component, Man et al.[6] reported that the physical aging of the film in the presence of a poling field only influenced the initial fast decay of the SHG on termination of poling and had little effect on the subsequent slow decay process; i.e., aging decreases free volume. The intermediate decay rate of the SGH signal is attributed to fluctuations in the size of free volume in the vicinity of each chromophore and is a strong function of temperature. The final quasi-stable stage of the SHG signal is mainly due to the persistence of the poling-field-induced, local, anisotropic environment below the T_g. Because of the strong coupling between the side-chain chromophores and polymer segments, some degree of alignment of the NLO chromophores will be retained in the anisotropic environment. The relaxation rate of this local, anisotropic environment mainly depends on the translational motion of the polymer segments, which is extremely restricted in the glassy state. In fact the residual SHG signal for many side-chain NLO polymers can be retained for several months.[6,8]

From the above considerations, we would predict that, if the polymer segments do not undergo anisotropic rearrangement under the poling field, the orientational order of the side-chain NLO dipoles created by the poling field will relax back to zero in a short period of time. One way to reduce the extent of the polymer segmental rearrangement under the poling field is to keep the poling temperature well below the T_g. Figure 5 shows an experiment in which the three SHG relaxation processes of the same sample at the same temperature (83 °C) were recorded. The only distinction among them is the different poling temperatures. When the sample was poled at 190 °C (23 °C above the T_g), the relatively large SHG signal was retained for a long period of time in the subsequent relaxation process. In the case of poling the sample at 161 °C (close to T_g), the magnitude of the retained SHG signal was reduced in the relaxation process relative to the one with poling above T_g. When the sample was poled at 124 °C (43 °C below the T_g and negligible chain contour rearrangement), the SHG signal relaxed to almost zero within a short period of time. This relaxation experiment is also consistent with the proposed concept of a poling-field-induced, anisotropic chromophore environment derived from a rearrangement of the polymer chain contours.

4.3. (Semi)quantitative Analysis of SHG Decay. A considerable amount of discrepancy concerning the analysis of the SHG decay data is present in the literature. Currently two functions are commonly used to fit the relaxation data for both the side-chain systems and the guest–host systems. One is the single Kohlrausch–Williams–Watts (KWW) stretched-exponential function (eq 1)[20] and another is the biexponential function (eq 2).[10,11] It should be mentioned that, over a very limited time scale, several functions may fit the relaxation data equally well. The particular function chosen depends on the proposed mechanism. A single mode mechanism requires a single mode function, e.g., either a single exponential or a single stretched exponential. In contrast a multimode mechanism requires a sum of contributing terms. Wang et al.[7] used a double KWW stretched-exponential function to fit the decay data for the sample of DANS dispersed in PMMA and ended up with the conclusion that both β_1 and β_2 are close to unity.

Based on our description for the entire relaxation process, a good fitting function should emphasize multimode relaxation. In our experiments quantitative information about the initial very rapid decay cannot be obtained because of the discharging operation (placing the top cover ITO slide on the sample to remove the surface charge). So that in our data fitting procedure, the initial fast decay data points were neglected and two slower modes were dominant: an intermediate relaxation and a very slow relaxation. Since the slowest modes of relaxation are so slow on our observation time scale, fitting the data collected over a few minutes to several hours of time cannot give accurate fitting parameters. Consequently, we simply used a constant to represent the slowest mode of relaxation at temperatures well below T_g. Thus the function given by eq 8 was adopted to fit the decay data.

Parts A–D of Figure 6 depict the relaxation data observed at 81, 102, 124, and 137 °C, respectively. In each case the sample was poled at 167 °C for 40 min. The comparison between the observed data points and the fitting curves (solid lines) with the fitting parameters summarized in Table 2 is also presented. Table 2 shows that the values of β decrease with the increasing relaxation temperature. This result is contradictory to the results obtained when a single KWW stretched function was used to fit the relaxation data.[20] As the temperature approached T_g, the relaxation rate of the slowest mode increases. Its contribution to the overall SHG relaxation can no longer be represented by a constant in eq 8. Consequently, contributions from the slowest relaxation mode begin to be manifested in the first term of eq 8. This is the reason why at 137 °C the relaxation time, instead of continuing to further decrease, begins to increase (Table 2). Quantitative analysis of the relaxation behavior based on the new mechanism that explicitly considers rearrangement of polymer segments in addition to chromophore mobility is in progress, and the results will be published in the future.

5. Conclusions

Electric field poling dynamics of a side-chain NLO polymer was studied along with the side-chain NLO chromophore orientational relaxation processes in the absence of poling field. A direct correlation between the poling conditions and the subsequent SHG relaxation behavior was evident. A biexponential function suggesting two dominant modes of orientation was used to fit the poling data. Surface charge dissipation effects on SHG relaxation were eliminated by grounding the sample surface. A qualitative mechanism that considers the anisotropic rearrangement of polymer backbone segments in the environment of the orientationally biased side-chain chromophores during the electric field poling process was proposed to interpret the poling and the subsequent relaxation behavior of the SHG signal. The proposed mechanism accounts for the influence of the electric-field-induced, local, anisotropic environment on the NLO chromophore's orientational relaxation behavior. The chromophore local environmental changes during the poling process were detected by a field-jump experiment.

Our interpretations of the observed SHG relaxation indicated that design strategies which enhance the intrinsic environmental anisotropy (e.g., liquid crystalline order) will be valuable for maintaining second-order NLO properties. Hence, systems that exhibit a strong coupling between the chromophore and its anisotropic environment would be good candidates for the next generation of NLO materials.

Acknowledgment. We thank Dr. Moon Young Jin and Mr. Mark Pauley for their preliminary work on setting up SHG measurement, Prof. Joe DeSimone for many helpful discussions, and Mr. Earl Danielson for help with the setup of the computer interfacing. This work is supported by Wright Patterson Materials Lab under Air Force Prime Contract F3361-90-C-5813.

References and Notes

(1) Godovsky, Y. K. *Thermophysical Properties of Polymers*; Springer-Verlag: Berlin, Germany, 1992.
(2) Struik, L. C. E. *Physical Aging in Amorphous Polymers and Other Materials*; Elsevier: Amsterdam, The Netherlands, 1978.
(3) Meredith, G. R.; Van Dusen, J. G.; Williams, D. J. *Macromolecules* **1982**, *15*, 1385.
(4) (a) Williams, D. J., Ed. Nonlinear Optical Properties of Organic and Polymeric Materials. ACS Symp. Ser. **1983**, *233*. (b) Prasad, P. N., Ulrich, D. R., Eds. *Nonlinear Optical and Electroactive Polymers*; Plenum: New York, 1988. (c) Chemla, D. S., Zyss, J., Eds. *Nonlinear Optical Properties of Organic Molecules and Crystals*; Academic: New York, 1987; Vol. 1. (d) Prasad, P. N.; William, D. J. *Introduction to Nonlinear Optical Effects in Molecules and Polymers*; John Wiley & Sons: New York, 1991.
(5) Singer, K. D.; Sohn, J. E.; Lalama, S. *J. Appl. Phys. Lett.* **1986**, *49*, 248.
(6) Man, H. T.; Yoon, H. N. *Adv. Mater.* **1992**, *4*, 159.
(7) Goodson, T., III; Wang, C. H. *Macromolecules* **1993**, *26*, 1837.
(8) Lindsay, G. A.; Henry, R. A.; Hoover, J. M.; Knoesen, A.; Mortazavi, M. A. *Macromolecules* **1992**, *25*, 4888.
(9) Singer, K. D.; King, L. A. *J. Appl. Phys.* **1991**, *70* (6), 3251.
(10) Hampsch, H. L.; Yang, J.; Wong, G. K.; Torkelson, J. M. *Macromolecules* **1990**, *23*, 3640.
(11) Hampsch, H. L.; Yang, J.; Wong, G. K.; Torkelson, J. M. *Macromolecules* **1990**, *23*, 3648.
(12) (a) Kohlrausch, R. P. *Ann. Phys.* **1854**, *1*, 179. (b) William, G.; Watts, D. C. *Trans. Faraday Soc.* **1970**, *66*, 80. (c) Torell, L. M.; Boerjesson, L.; Elmroth, M. *J. Phys., Condens. Matter* **1990**, *2*, SA207. (d) Scher, H.; Schlesinger, M. F.; Bendler, J. *Phys. Today* **1991**, Jan.
(13) Wang, H.; Jarnagin, R. C.; Samulski, E. T.; DeSimone, J., to be published.
(14) Kurtz, S. K.; Jerphagnon, J.; Choy, M. M.; Landolt-Bornstein, *Numerical Data and Functional Relationships in Science and Technology*; Springer: New York, 1979; Vol. 11, p 671.
(15) Jerphagnon, J.; Kurtz, S. K. *J. Appl. Phys.* **1970**, *41* (4), 1667.
(16) Krause, S.; O'Konski, C. T. In *Molecular Electro-Optics*; Krause, S., Ed.; Plenum Press: New York, 1980.
(17) Eich, M.; Sen, A.; Looser, H.; Bjorklund, G. C.; Swalen, J. D.; Twieg, R.; Yoon, D. Y. *J. Appl. Phys.* **1989**, *66* (6), 2559.
(18) Kuzyk, M. G.; Moore, R. C.; King, L. A. *J. Opt. Soc. Am. B* **1990**, *7*, 64.
(19) Wang, C. H.; Guan, H. W., private communication.
(20) Walsh, C. A.; Burland, D. M.; Lee, V. Y.; Miller, R. D.; Smith, B. A.; Twieg, R. J.; Volksen, W. *Macromolecules* **1993**, *26*, 3720.
(21) Singer, K. D.; Sohn, J. E.; Kuzyk, M. G. *J. Opt. Soc. Am. B* **1987**, *4*, 968.
(22) Kuzyk, M. G.; Singer, K. D.; Zahn, H. Z.; King, L. A. *J. Opt. Soc. Am. B* **1989**, *6*, 742.
(23) Van der Vost, C. P.; Picken, S. J. *SPIE Conf. Proc.* **1987**, *866*, 99.
(24) Mohlman, G. R.; Van der Vorst, C. P. In *Side Chain Liquid Crystal Polymers*; McArdle, C. B., Ed.; Blackie and Son: Glasgow, Scotland, 1989; p 330.
(25) Moreno, R. A.; Gross, B. *J. Appl. Phys.* **1976**, *47* (8), 3397.
(26) Curro, J. G.; Lagasse, P. R.; Simha, R. *Macromolecules* **1982**, *15*, 1621.
(27) Deloche, B.; Samulski, E. T. *Macromolecules* **1981**, *14*, 578.
(28) Toriumi, H.; Deloche, B.; Herz, J.; Samulski, E. T. *Macromolecules* **1985**, *18*, 304.
(29) Deloche, B.; Samulski, E. T. *Macromolecules* **1988**, *21*, 3107.
(30) Warner, M. In *Side Chain Liquid Crystal Polymers*; McArdle, C. B., Ed.; Chapman and Hall: New York, 1989; p 7.
(31) Noirez, L.; Cotton, J. P.; Hardouin, F.; Keller, P.; Moussa, F.; Pepy, G.; Strazielle, C. *Macromolecules* **1988**, *21*, 2889.
(32) Percec, V.; Hahn, B.; Ebert, M.; Wendorff, J. H. *Macromolecules* **1990**, *23*, 2092.